

Theoretical study of the role of solvent Stark effect in electron transitions

M. Elena Martín · M. Luz Sánchez · José C. Corchado · Aurora Muñoz-Losa · Ignacio Fdez. Galván · Francisco J. Olivares del Valle · Manuel A. Aguilar

Received: 5 July 2010/Accepted: 14 October 2010/Published online: 30 October 2010
© Springer-Verlag 2010

Abstract The possible influence of the solvent Stark effect (SSE) on the solvatochromic shift in electron transitions has been analyzed by using the ASEP/MD (averaged solvent electrostatic potential from molecular dynamics) method. With this purpose, four molecules, two polar (acrolein and formaldehyde) and two non-polar (*p*-difluorobenzene and *trans*-difluoroethene) have been studied in solvents of diverse polarity. Independently of the nature of the system we found that the contribution of SSE on the average value of the solvent shift or on the multipole moment values is negligible. In the case of centro-symmetric molecules, our results permit to discard the SSE as cause of the solvent shift found, which must be assigned to the electrostatic interaction of the solute quadrupole and higher multipoles with the solvent. As the SSE values provide also a measure of the errors introduced by the mean field approximation (MFA), these results indicate that MFA permits a very accurate determination of the solvent shift at the same time that it reduces drastically the computational cost. Finally, a new procedure suited to the ASEP/MD method has been presented that permits to estimate the inhomogeneous broadening of spectral bands, complementing the information provided by mean field theories. This procedure does not need additional quantum calculations and its computational cost is minimal.

Published as part of the special issue celebrating theoretical and computational chemistry in Spain.

M. E. Martín · M. L. Sánchez · J. C. Corchado · A. Muñoz-Losa · I. Fdez. Galván · F. J. Olivares del Valle · M. A. Aguilar (✉)
Química Física, Edif. José María Viguera Lobo,
Universidad de Extremadura, Avda. de Elvas s/n,
06071 Badajoz, Spain
e-mail: maguilar@unex.es

Keywords Solvent Stark effect · ASEP/MD · QM/MM · Mean field theories

1 Introduction

When a solute is transferred from the vacuum to a solvent, the shift in the position of the absorption bands of the corresponding electronic spectra is due to the differential interaction of the ground and excited states with the solvent. The two main components of the interaction energy that contribute to this solvent shift are the always present dispersion term and the possible change in the dipole moment of the solute during the excitation. Other terms, such as for instance, solvent Stark effect (SSE) [1, 2] or that due to the interaction of the quadrupole and higher multipole moments of the solute with the solvent are considered less important.

The solvent Stark effect is the stabilizing energy associated to the interaction between the fluctuating electric field originated by the solvent thermal movements and the induced dipole moment in the solute molecule, and, at first order, it is proportional to the solute polarizability and to the fluctuations of the solvent electric field. This component contributes to the solvent shift of polar and non-polar solutes, although one expects that its effect will be proportionally larger in non-polar solutes. In the last years [3], there has been a certain controversy about the role that the solvent Stark effect plays in the explanation of solvent effects of centro-symmetric molecules where the dipole interaction vanishes. Other explanations about the origin of the solvent shift of these molecules are the interaction of the quadrupole and higher multipole moments of the solute with the solvent [3] and the hardly probable existence, because of symmetry considerations, of small dipole moments in the excited states [4].

Solvent Stark effect plays also an important role in the comparison between different solvent effects theories as its value permits to evaluate the accuracy of the mean field approximation (MFA) [5]. This approximation is at the core of some of the more profusely used solvent effect theories: dielectric continuum models in their different quantum versions [5–11], Langevin dipoles models [12], etc. One of the main problems that face solvent effect theories is the great number of solvent configurations that are thermally accessible. In general, different solute molecules will have different environments and, consequently, slightly different properties. In order to obtain statistically significant results, it is necessary to include hundreds or thousands of solute–solvent configurations. If, as usual, the solute is quantum-mechanically represented, that means to perform several hundreds or thousands of quantum calculations [12–21]. MFA permits to drastically reduce the number of quantum calculations. In MFA, one does not consider the effect of specific configurations; instead, the solvent perturbation is included in an averaged way. The available theories differ in the way the solvent perturbation is obtained. So, if the solvent is described as a dielectric, we get the different continuum theories. Other descriptions of the solvent are also possible: as a conductor, using Langevin dipoles, or molecular mechanics force fields. In the latter case, the solvent structure can be obtained using RISM theory [22], Monte Carlo or molecular dynamics (MD) simulations [23, 24]. In the model proposed in our laboratory, named ASEP/MD, acronym for Averaged Solvent Electrostatic Potential from Molecular Dynamics [25], the solvent structure is obtained from MD simulations and the solvent perturbation is described using potential fitted charges. Since in MFA the solvent perturbation enters in an averaged way into the solute molecular Hamiltonian, this approximation completely neglects the correlation between the motion of the solvent molecules and the response of the solute electron polarizability, i.e., MFA does not allow the solute to polarize in response to a change in the solvent configuration. In other words, MFA completely neglects the solvent Stark effect.

In the present study, we will try to respond to the following questions related to the SSE: (a) Does SSE play any role in the description of the solvent shift of centro-symmetric molecules or, on the contrary, is the interaction of the quadrupole and higher multipole moments of the solute with the solvent responsible for the solvent shift? (b) Given that SSE is a function of the fluctuations of the solvent electric field and these could be affected by the solute–solvent interaction, is SSE affected by the nature, polar or non-polar, of the solute? (c) Under which conditions is SSE negligible? Or in other words, when is MFA a good approximation?

In order to answer these questions, two sets of solutes (polar and non-polar) were studied in three solvents of diverse polarity. The in-solution transition energies to the first electronic excited states were calculated with the ASEP/MD methodology and by comparison with the in-vacuum transitions, the solvent shift value was evaluated. Next, our interest was focused in the origin of this shift, paying special attention to the possible contribution of the solvent Stark Effect to the total solvent shift.

Finally, we have also tackled an additional question related to the contribution of the SSE to the inhomogeneous bandwidth. A limitation of the solvent theories that make use of MFA is that they provide a specific value for the solvent shift or for the maximum of the absorption and emission bands but not for the inhomogeneous broadening of the spectral bands. In the case of ASEP/MD, this limitation can be easily corrected using the solvent configurations obtained along the ASEP/MD procedure. Comparison with the results obtained with more conventional QM/MM methods permits us to evaluate the effect that the instantaneous polarization of the solute has on the bandwidth.

The rest of the paper is organized as follows: The Sect. 2 covers a brief outline of the ASEP/MD methodology (Sect. 2.1) for subsequently dealing with more detail with its application in the estimation of the SSE (Sect. 2.2) and the bandwidth for the absorption spectrum bands (Sect. 2.3). The Sect. 3 presents the complete description of the carried out calculations, and the results will be collected in the Sect. 4. Finally, the Sect. 5 brings together the conclusions.

2 Method

2.1 The ASEP/MD method

The ASEP/MD method is a sequential QM/MM method that alternates full MD simulations with quantum mechanics calculations and that uses the MFA. From each classical MD simulation, the averaged electrostatic solvent potential is obtained and the properties of the solute molecule are quantum-mechanically calculated in the presence of this potential. The new polarized solute charge distribution can perturb the solvent structure around it and consequently the process has to be re-started performing a new MD simulation and getting a new averaged solvent potential. The iterative process must continue until convergence is achieved and the solvent structure is equilibrated with the electronic distribution of the solute. This method has been successfully employed in the study of a great variety of chemical processes, such as conformational equilibrium [26], chemical reactivity [27], and non-radiative excited state decay [28, 29]. Another field where ASEP/MD has demonstrated its utility has been in the

study of the solvent effects on the absorption and emission bands of electronic spectra [30–33]. The method is able to evaluate the solvent shift originated by the electrostatic and polarization components of the solute–solvent interaction energy. Some details of the method pertinent to the current research can be found elsewhere [25, 34–37].

2.2 Estimation of the solvent Stark effect

Solvent theories that use the mean field approximation completely neglect the contribution of the solvent Stark effect. Consequently, for the determination of this error in the absorption process, we must compare the transition energy when the MFA is used and when it is not. In a previous article [37], we determined the contribution of the SSE to the energy and several electric properties of molecules in solution. This contribution turned out to be minimal, representing less than 5% of the solute–solvent interaction energy and 1% of the solute dipole moment. In that paper, we also proposed a perturbational expression that recovered part of the SSE contribution. Results showed that the errors in the energy could be reduced to 2.5%. A recent paper [38] has estimated the effect of SSE on reaction rates in about 5%. Once the use of MFA for ASEP/MD has been verified to give correct results in the study of different properties on molecules in their ground states, our aim in this paper is to check the validity of this approximation in the study of processes where excited states are implied.

As it is usual in QM/MM methods, the Hamiltonian is partitioned in the following way:

$$\hat{H} = \hat{H}_{\text{QM}} + \hat{H}_{\text{MM}} + \hat{H}_{\text{QM/MM}} \quad (1)$$

with terms that correspond to the quantum part, \hat{H}_{QM} , the classical part, \hat{H}_{MM} , and to the interaction between them, $\hat{H}_{\text{QM/MM}}$. The energy and state function of the solvated solute molecule are obtained by solving, for each configuration, the effective Schrödinger equation:

$$(\hat{H}_{\text{QM}} + \hat{H}_{\text{QM/MM}})|\Psi\rangle = E|\Psi\rangle \quad (2)$$

Even though the interaction Hamiltonian has electrostatic and non-electrostatic contributions, the SSE mainly comes from the electrostatic term. In QM/MM methods, the electrostatic contribution is:

$$\hat{H}_{\text{QM/MM}}^{\text{elect}} = \int dr \cdot \hat{\rho} \cdot V_{\text{S}}(r; X_i) \quad (3)$$

where $\hat{\rho}$ is the solute charge density, $V_{\text{S}}(r; X_i)$ the electrostatic potential generated at the position r by the solvent molecules at the configuration X_i . In that case, the Schrödinger equation has to be solved for each one of the N configurations selected from an MD simulation. The

system properties are then obtained by averaging over the N configurations:

$$\langle A \rangle = \frac{1}{N} \sum_{i=1}^N A(X_i) \quad (4)$$

However, when the MFA is used, the term for the electrostatic potential of the Hamiltonian reads:

$$\hat{H}_{\text{QM/MM}}^{\text{elect}} = \int dr \cdot \hat{\rho} \cdot \langle V_{\text{S}}(r) \rangle \quad (5)$$

where the bracket denotes a statistical average. The term $\langle V_{\text{S}}(r) \rangle$ is known as the averaged solvent electrostatic potential (ASEP). Solving the Schrödinger equation (2) with the solute–solvent interaction Hamiltonian (5), the energy, E_{MFA} , and wave function, Ψ_{MFA} , of the solute perturbed by the solvent are obtained. This approximation permits a drastic reduction of the computational cost associated to the determination of solvent shifts.

When studying electron transitions, there are two solute electronic states involved; each of them has a distinct energy and SSE. The SSE for each state is calculated as:

$$W_{\text{Stark}}^X = \langle E^X \rangle - E_{\text{MFA}}^X \quad (6)$$

where the superscript X is ex for the excited state and g for the ground state and $\langle E \rangle$ and E_{MFA} are calculated with Eqs. (1)–(4) and (1), (2), and (5), respectively.

Finally, the solvent Stark effect on the transition energy can be evaluated as the difference between the SSE at the excited and ground states:

$$\Delta W_{\text{Stark}} = W_{\text{Stark}}^{\text{ex}} - W_{\text{Stark}}^g = \langle \Delta E \rangle - \Delta E_{\text{MFA}} \quad (7)$$

where $\langle \Delta E \rangle$ and ΔE_{MFA} are transition energies calculated without or with the MFA, respectively.

Once the transition energies in vacuum and in solution are known, the calculation of the solvent shift (δ) is immediate:

$$\delta_{\text{MFA}} = \Delta E_{\text{MFA}} - \Delta E^0 \quad (8)$$

where ΔE^0 is the transition energy in vacuum and ΔE_{MFA} is the in-solution corresponding term calculated by making use of MFA. Analogous expression can be obtained for $\langle \delta \rangle$ if the in-solution transition energy is calculated as an average of quantum calculations, $\langle \Delta E \rangle$.

2.3 Estimation of the bandwidth

Due to the use of an average configuration, mean field theories do not provide any information about the statistical distribution of excitation energies. However, in many occasions, it could be interesting to have some data not only on the position of the maximum but also on the bandwidth associated to the thermal agitation of the solvent, the so named inhomogeneous broadening. Although this is a

general limitation of MFA theories, in the particular case of ASEP/MD it can be easily corrected because ASEP/MD can generate as output the microscopic distribution of solvent molecules around the solute. With this information, an estimation of the transition energy distribution can be easily obtained. The procedure is as follows: at the end of the ASEP/MD process, we calculate the product between the molecular electrostatic potential generated by the solute wavefunction at the positions occupied by the solvent molecules (in the configuration X_i) and the atomic solvent charges. This permits to calculate the solute–solvent interaction energy for the ground, $E_{\text{s-S}}^{\text{g}}$, and excited, $E_{\text{s-S}}^{\text{ex}}$, states. ASEP/MD also provides the QM energy of the solute molecule, by assembling all terms we get the transition energy when the solvent is at the X_i configuration:

$$\Delta E_{\text{MFA}}(X_i) = \langle \Psi_{\text{MFA}}^{\text{ex}} | H^0 | \Psi_{\text{MFA}}^{\text{ex}} \rangle - \langle \Psi_{\text{MFA}}^{\text{g}} | H^0 | \Psi_{\text{MFA}}^{\text{g}} \rangle + E_{\text{s-S}}^{\text{ex}}(X_i) - E_{\text{s-S}}^{\text{g}}(X_i) \quad (9)$$

It is worth noting that in our approximation the solute response to the changes in the solvent distribution as a consequence of the thermal agitation is neglected. Finally, by comparing this result to that obtained when this limitation is released (using a different solute charge distribution for each solvent configuration, as it is done in other QM/MM methods), one can get an estimation of the SSE on the band broadening.

3 Computational details

Electronic transition energies in vacuum and in solution were calculated for acrolein, formaldehyde, *p*-difluorobenzene (*p*-DFB), and *trans*-difluoroethene (*trans*-DFE). The first two molecules are polar and the others non-polar. Water, methanol, and cyclohexane were the chosen solvents for this study as they span a broad range of polarity.

The in-solution calculations were carried out with the ASEP/MD method. As it has been said before, ASEP/MD combines in an alternated way quantum calculations and MD simulations. In this study, Gaussian 98 [39] was the quantum package of programmes used during the ASEP/MD iterative process whereas Moldy [40] was the program employed for the MD simulations. The solute molecule was allowed to relax its intramolecular geometry in solution and in this way at the end of the ASEP/MD iterative process the solvent structure and the electronic and geometric distribution of the solute become mutually equilibrated. Two quantum calculation levels were employed in the geometry optimization, Møller-Plesset (MP2) [41] and Complete Active Space Self Consistent Field (CASSCF) [42] methods. Nevertheless, it has been proved [43] that electron transition energies can only be given with accuracy

when dynamic electron correlation is included, with a method such as CASPT2 [44, 45]. Consequently, independently of the level of calculation used for the geometry optimization, all the transition energies collected in this paper were calculated by using the CASPT2 method available in the MOLCAS [46] program.

Different active spaces have been used for each of the studied systems in water solution. For acrolein and formaldehyde, the complete active space method was employed both for the optimization as for the transition energy calculation. These spaces include the total π structure and the lone pairs of the oxygen atom for the occupied space and the corresponding anti-bonding π^* orbitals for the virtual space. The calculation levels are displayed in Table 1.

For acrolein and formaldehyde, the first excited state corresponds to an ($n-\pi^*$) state where one of the electrons of the oxygen lone pairs is promoted to the first anti-bonding π^* orbital. On the contrary, *p*-DFB and *trans*-DFE present a first excited state corresponding to a ($\pi-\pi^*$) transition. Except for *p*-DFB where a state average of ten roots was employed in the calculation of the vertical excitation, a state average of two roots, including the ground and the first excited state, was considered for the rest of the solutes.

In view of the results obtained in water solution, only a reduced number of calculations were performed in methanol. In particular, only non-polar solutes with MP2 geometry optimization were studied and the smaller active spaces were selected for energy calculations. Finally, and with the aim of comparing the evolution of the transition energies

Table 1 Calculation levels used in this work for the different solute/solvent combinations

	Vacuum and water	Methanol	Cyclohexane
Acrolein	CASPT2(6,5)// CASSCF	–	–
Formaldehyde	CASPT2(4,3)// CASSCF	–	–
<i>p</i> -DFB	CASPT2(10,8)// CASSCF CASPT2(6,6)// CASSCF CASPT2(6,6)// MP2	CASPT2(6,6)// MP2 CASPT2(6,6)// MP2	CASPT2(6,6)// MP2
<i>trans</i> -DFE	CASPT2(2,2)// CASSCF CASPT2(6,4)// MP2 CASPT2(2,2)// MP2	CASPT2(2,2)// MP2 CASPT2(2,2)// MP2	–

The active space includes always the π space of the solute and the lone pairs of the oxygen or fluorine atoms, except for the lower active spaces of *trans*-DFE and *p*-DFB, where the lone pairs are not included; the active space of the CASSCF method is always the same as for CASPT2

and solvent shift of a non-polar solute when transferred to solvents of different polarity, a CASPT2(6,6)/MP2 calculation of *p*-DFB was performed as well in cyclohexane.

Molecular dynamics simulations were carried out with Moldy and were designed as follows. The system was considered as an assembly of rigid molecules where one solute molecule was introduced in a cubic box surrounded by a large enough number of solvent molecules to ensure the adequate representation of the system in solution. The number of solvent molecules in each simulation varies with the solute size and with the solvent nature between 215 and 360. The geometries of cyclohexane and methanol were optimized with B3LYP/6-311G** and their Lennard-Jones parameters were taken from the OPLS-AA [47] force field. The same choice was made for the Lennard-Jones parameters of the different solutes. For water, the TIP3P [48] model was employed. Periodic boundary conditions were applied and spherical cutoffs were used to truncate the interatomic interactions. These cutoffs were approximately 10 Å in water solution and around 13 Å for methanol and cyclohexane solvents. Long-range interactions were calculated using the Ewald sum technique [23] and the temperature was fixed at 298 K by using the Nosé-Hoover thermostat [49]. Each simulation was run for 150,000 time steps, where 50,000 were for equilibration and 100,000 for production. A time step of 0.5 fs was used.

At each step of the ASEP/MD procedure, 100 configurations evenly distributed along the MD run were used to calculate the ASEP and to represent the solvent effect in the quantum geometry optimization of the solute. The ASEP/MD process continued until the energies and solute geometry were stable for at least five iterations.

When the ASEP/MD procedure finishes, transition energies and solvent shift values obtained in the presence of an average solvent configuration are available. The last MD simulation from each of the previously described ASEP/MD calculations was used for running a second set of calculations. For this, a total of 100 evenly distributed solvent configurations were selected from each final simulation, and using the same active space as with ASEP/MD, 100 CASPT2 quantum calculations were run for each case. Averaging over the 100 transition energies obtained in solution, a new averaged transition energy, $\langle \Delta E \rangle$, was given that accounts for the instantaneous interaction between solute and solvent.

4 Results

4.1 Solvent Stark effect on the solvent shifts

MP2 and/or CASSCF optimized geometries were used for the calculation of the vertical transition energies to the first

excited state for each molecule. CASPT2 level of calculation and appropriate active space were employed for energy calculations. The most representative internal parameters obtained after the in-vacuum and in-solution optimizations are presented in Table 2. See Fig. 1 for parameter identification. As it could be predicted, no dramatic changes are observed when the solute is transferred from vacuum to solution. The trend in bond lengths agrees with the results obtained in previous studies, that is, double bonds tend to become longer and adjoining single bonds shorter than in vacuum conditions. Practically no changes are observed in the benzene ring of *p*-DFB. Roughly, variations are equivalent in water and methanol solvents and practically negligible in cyclohexane. Comparing different levels of calculation, for *p*-DFB and *trans*-DFE in water, it can be observed that CASSCF provides shorter bond lengths than MP2 both in vacuum and in solution. This fact has been already noted in previous studies [32].

Table 3 compares the in-vacuum vertical excitation energies and the available experimental data [50–55]. In general, good agreement can be observed between both sets of values. It is remarkable that the use of different levels of calculation, CASSCF or MP2, in optimizing the geometries gives negligible variations in transition energies. The larger discrepancy with the experiment is displayed by *trans*-DFE. This fact can be a consequence of different causes like, for instance, the neglect of the quite close Rydberg states corresponding to the transitions to the 3s and 3p Rydberg orbitals [56]. However, given that our main aim is the estimation of the solvent shift that is calculated as a difference of transition energies and that it is not expected that Rydberg states contribute in any appreciable way to the in-solution spectra, we did not try to improve this value.

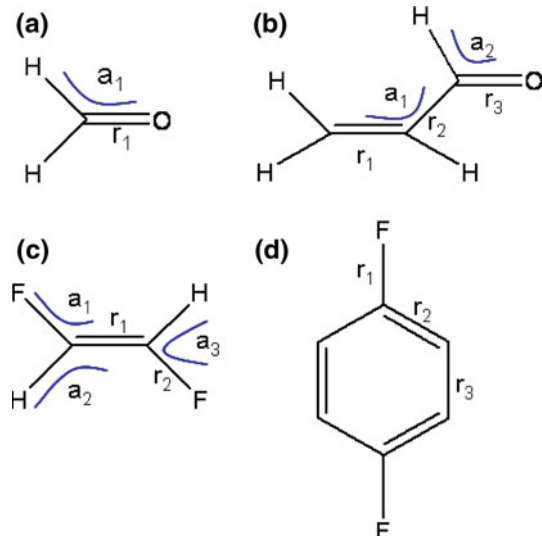
Oscillator strengths (OS) are displayed in Table 4. (n–π*) transitions are dipole-forbidden and consequently OS for acrolein and formaldehyde are negligible. The HOMO–LUMO transition studied for *p*-DFB is a (π–π*) transition and it presents also a very low OS value as a consequence of being a dipole-forbidden transition. Nevertheless, these bands, even though with very low intensity, appear in the UV spectra due to vibronic coupling. The case is different for the *trans*-DFE first (π–π*) excited state, the high value of the OS shows this state as a bright one.

Transition energies in solution are collected in Table 5. Given the nature of the transitions considered, transition energies are systematically larger in solution than in vacuum, and consequently, the solvent effect results always in a blue shift. As expected, the magnitude of the solvent shift increases with the polarity of the solute and the solvent, passing from 0.2 kcal/mol for *p*-DFB in cyclohexane to 5.2 kcal/mol for acrolein in water solution. The main point to remark is the practical coincidence between $\langle \delta \rangle$ and δ_{MFA} and, consequently, the exceedingly small contribution

Table 2 Selected geometrical parameters in vacuum (*V*) and in solution (*S*). Water for the top half

Formaldehyde		<i>trans</i> -Difluoroethene				<i>p</i> -Difluorobenzene				Acrolein				
CASSCF(4,3)		CASSCF(2,2)		MP2		CASSCF(10,8)		CASSCF(6,6)		MP2		CASSCF(6,4)		
<i>V</i>	<i>S</i>	<i>V</i>	<i>S</i>	<i>V</i>	<i>S</i>	<i>V</i>	<i>S</i>	<i>V</i>	<i>S</i>	<i>V</i>	<i>S</i>	<i>V</i>	<i>S</i>	
<i>r</i> ₁	1.198	1.203	1.326	1.335	1.329	1.359	1.333	1.340	1.337	1.431	1.358	1.365	1.340	1.339
<i>r</i>			1.331	1.070	1.354	1.083	1.388	1.386	1.388	1.386	1.390	1.388	1.473	1.464
<i>r</i> ₃						1.396	1.395	1.397	1.395	1.396	1.395	1.204	1.210	
<i>a</i> ₁	121.62	121.29	119.57	119.08	119.77	119.11						121.65	120.51	
<i>a</i> ₂			125.65	126.28	125.38	126.23						120.36	119.77	
<i>a</i> ₄			114.78	114.65	114.85	114.66								
Methanol														
<i>trans</i> -Difluoroethene				<i>p</i> -Difluorobenzene				<i>p</i> -Difluorobenzene						
MP2		MP2		MP2		MP2								
<i>V</i>	<i>S</i>	<i>V</i>	<i>S</i>	<i>V</i>	<i>S</i>	<i>V</i>	<i>S</i>							
<i>r</i> ₁	1.329	1.357	1.358	1.361	1.358	1.357								
<i>r</i> ₂	1.354	1.084	1.390	1.389	1.390	1.390								
<i>r</i> ₃			1.396	1.395	1.396	1.395								
<i>a</i> ₁	119.77	119.27												
<i>a</i> ₂	125.38	126.00												
<i>a</i> ₃	114.85	114.73												

Distances in ångströms, angles in degrees

**Fig. 1** Geometrical parameter identification. **a** Formaldehyde. **b** Acrolein. **c** *trans*-DFE. **d** *p*-DFB

(lower than 0.06 kcal/mol in all cases) of the SSE to the solvent shift independently of the nature, polar or non-polar, of the solute. Table 5 also displays $W_{\text{Stark}}^{\text{g}}$ and $W_{\text{Stark}}^{\text{ex}}$ values. It is worth remarking that the contributions of SSE to the solute–solvent interaction energies can be appreciably larger, with values that, in some cases, are close to 1 kcal/mol. However, given that ground and excited states display

Table 3 Transition energies in vacuum (in kcal/mol)

	$\Delta E^0 \text{ exp}$	$\Delta E^0 \text{ calc}^{\text{g}}$
Acrolein	85.6 ^a –86.5 ^b	83.1
Formaldehyde	87.4 ^c –93.8 ^d	92.3
<i>p</i> -Difluorobenzene	107.7 ^e	109.4–109.9
<i>trans</i> -Difluoroethene	171.8 ^f –174.3 ^d	187.9–190.6

^a Ref. [50], ^b Ref. [51], ^c Ref. [52], ^d Ref. [53], ^e Ref. [54], ^f Ref. [55], ^g CASPT2(6,5) calculation for acrolein and CASPT2(4,3) for formaldehyde. Transition energies for *p*-difluorobenzene: 109.4, 109.8, and 109.9 kcal/mol for CASPT2(10,8)/CASSCF(10,8), CASPT2(6,6)/CASSCF(6,6), and CASPT2(6,6)/MP2 calculations, respectively. Transition energies for *trans*-difluoroethene: 187.9, 190.4 and 190.6 kcal/mol for CASPT2(6,4)/MP2, CASPT2(2,2)/CASSCF(2,2), and CASTP2(2,2)/MP2 calculations, respectively

similar values of W_{Stark} , the final SSE contribution to the solvent shifts, Eq. (7), is completely negligible. In sum, one can conclude that MFA is a very good approximation that introduces only small errors in the calculation of solvent shifts. This conclusion seems valid independently of the nature of the solute (polar or non-polar) and of the solvent (protic or aprotic, polar or non-polar). At first order, the SSE contribution to the solvent shift is a function of the solvent electric field fluctuations in the ground state (only vertical absorptions where the FC principle is applicable were studied) and the difference between the solute polarizabilities in the ground and in the excited state. Given that all the

Table 4 In solution oscillator strengths

	Calculation	Oscillator strength
Water		
Acrolein	CASPT2(6,5)//CASSCF(6,5)	1.546E–06
Formaldehyde	CASPT2(4,3)//CASSCF(4,3)	6.229E–08
<i>p</i> -DFB	CASPT2(6,6)//CASSCF(6,6)	8.408E–03
	CASPT2(10,8)//CASSCF(10,8)	7.461E–02
	CASPT2(6,6)//MP2	4.886E–02
<i>trans</i> -DFE	CASPT2(2,2)//CASSCF(2,2)	4.887E–01
	CASPT2(6,4)//MP2	4.859E–01
	CASPT2(2,2)//MP2	4.886E–01
Methanol		
<i>p</i> -DFB	CASPT2(6,6)//MP2	5.748E–02
<i>trans</i> -DFE	CASPT2(2,2)//MP2	4.886E–01
Cyclohexane		
<i>p</i> -DFB	CASPT2(6,6)//MP2	6.676E–02

transitions considered in this study are valence transitions, one expects that the change in polarizability during the transition will be small. This explains the small values of SSE.

It seems also clear that SSE does not contribute in any significant way to the final value of the solvent shift in centro-symmetric molecules and that for this group of molecules electrostatic (quadrupole and higher multipoles) interactions are responsible for the observed solvent shift.

4.2 Solvent Stark effect on multipole moments

In this section, we will consider the SSE on the dipole and quadrupole moments of formaldehyde and acrolein

molecules at their ground and excited states. It will be shown that in the evaluation of these properties, the difference between the results provided by theories using or not MFA is as well negligible.

MFA provides dipole and quadrupole moment values very close to the average values obtained from the 100 quantum calculations set both for the ground and the excited states (see Table 6). This fact is illustrated in Fig. 2 where histograms of the statistical distribution of the dipole moment are displayed alongside with the dipole moment value calculated using MFA. For the sake of brevity, only the histograms corresponding to the ground and excited states of acrolein are shown being the conclusions obtained for the formaldehyde molecule completely equivalent. From the results collected in Table 6, it can be noted that there is a very good agreement between $\langle \mu \rangle$ and μ_{MFA} , and $\langle \theta \rangle$ and θ_{MFA} , with differences lower than 0.1 D in the

Table 6 Dipole moment (D) and quadrupole moment ($D \cdot \text{\AA}$) for formaldehyde and acrolein in their ground (S_0) and excited (S_1) states. ASEP/MD and average values from 100 calculations are showed

	$\mu(S_0)$	$\mu(S_1)$	$\theta(S_0)$	$\theta(S_1)$
Acrolein				
ASEP	3.93	1.84	−74.01	−73.31
Quantum 100	3.85	1.80	−73.93	−72.51
% Error	2.0	2.0	1.0	1.1
Formaldehyde				
ASEP	2.95	1.85	−34.22	−34.63
Quantum 100	2.99	1.89	−34.07	−34.55
% Error	1.0	2.0	0.4	0.23

Table 5 Solvent Stark effect (W_{Stark}), transition energies (ΔE) and solvent shift (δ) (in kcal/mol) calculated from ASEP/MD and as average of 100 quantum calculations

	Calculation	W_{Stark}			ΔE			δ	
		W_{Stark}^g	W_{Stark}^e	ΔW_{Stark}	$\langle \Delta E \rangle$	ΔE_{MFA}	ΔE^0	$\langle \delta \rangle$	δ_{MFA}
Water									
Acrolein	CASPT2(6,5)//CASSCF(6,5)	0.78	0.85	0.063	88.26	88.32	83.08	5.18	5.24
Formaldehyde	CASPT2(4,3)//CASSCF(4,3)	0.37	0.36	−0.006	95.79	95.79	92.30	3.49	3.49
<i>p</i> -DFB	CASPT2(6,6)//CASSCF(6,6)	0.77	0.77	−0.002	111.03	111.02	109.86	1.16	1.16
	CASPT2(10,8)//CASSCF(10,8)	0.80	0.81	0.005	110.58	110.58	109.40	1.18	1.18
	CASPT2(6,6)//MP2	0.79	0.80	0.001	111.16	111.16	110.02	1.14	1.14
<i>trans</i> -DFE	CASPT2(2,2)//CASSCF(2,2)	0.40	0.36	−0.037	191.96	191.92	190.42	1.54	1.51
	CASPT2(6,4)//MP2	0.42	0.48	0.059	189.68	189.74	187.92	1.75	1.81
	CASPT2(2,2)//MP2	0.36	0.33	−0.031	192.34	192.31	190.62	1.72	1.69
Methanol									
<i>p</i> -DFB	CASPT2(6,6)//MP2	0.40	0.40	0.000	110.66	110.66	110.02	0.64	0.64
<i>trans</i> -DFE	CASPT2(2,2)//MP2	0.19	0.16	−0.026	191.60	191.58	190.62	0.98	0.95
Cyclohexane									
<i>p</i> -DFB	CASPT2(6,6)//MP2	0.00	0.00	0.000	110.18	110.18	110.02	0.16	0.16

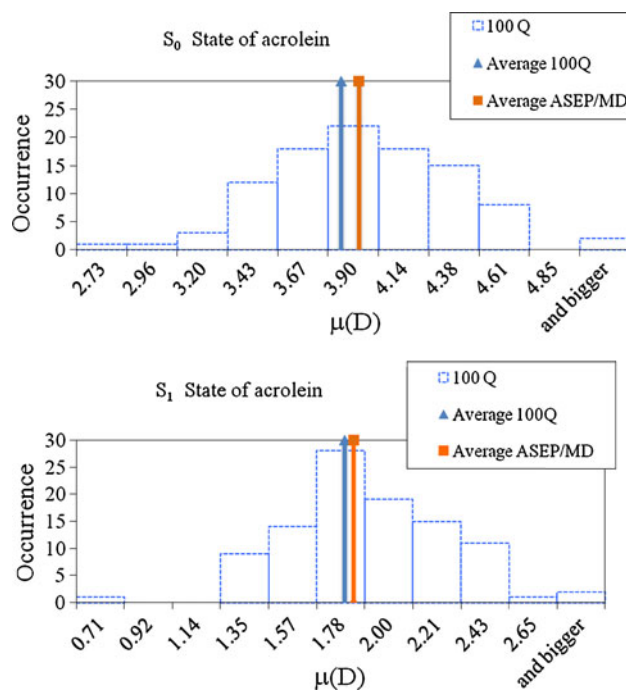


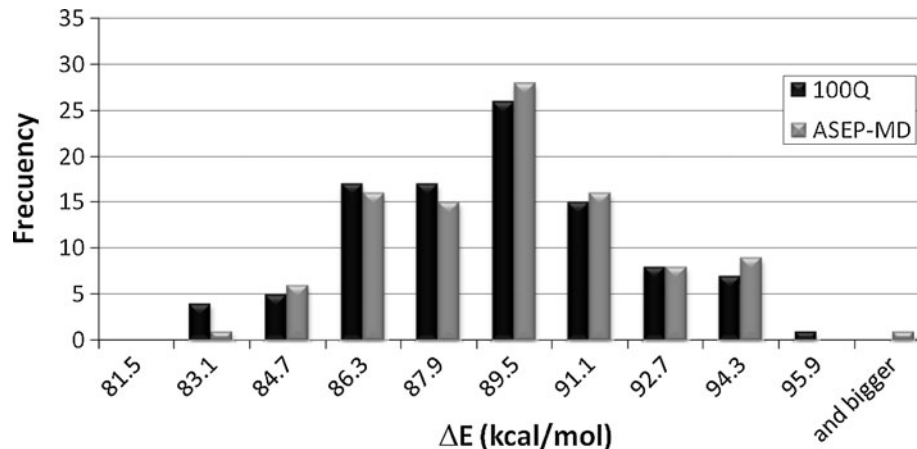
Fig. 2 Statistical distribution of the dipole moment (D) for acrolein from 100 quantum calculations. The central orange full line is the value obtained by using ASEP/MD. Ground and excited state dipole moments are represented

dipole values and 0.8 D° in the quadrupoles; these values represent an error lower than 2.5%. Consequently, it can be concluded that, as in the case of solvent shift, the use of MFA does not introduce significant errors in the calculation of electric properties of molecules in their ground and excited states.

4.3 Solvent Stark effect on inhomogeneous broadening

As it has been shown above, the use of MFA provides accurate results for the transition energies and multipole moments reducing at the same time the computational cost;

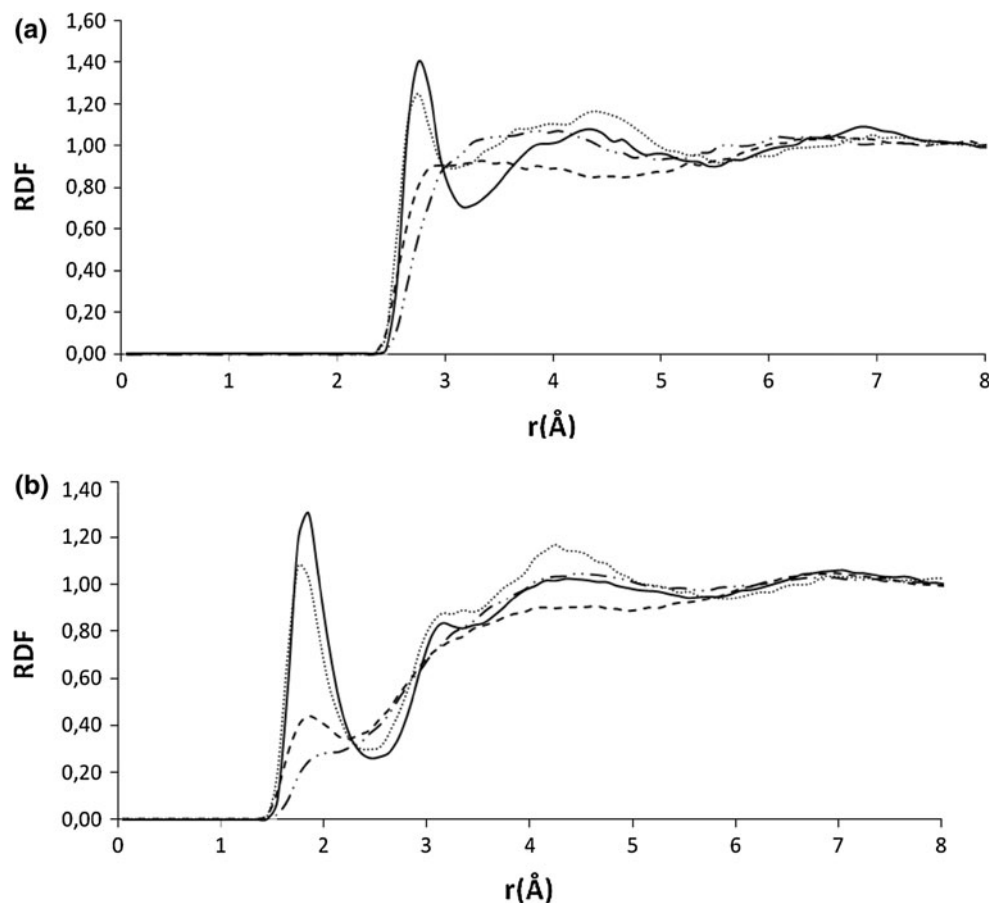
Fig. 3 Statistical distribution of ΔE (kcal/mol) for acrolein from 100 quantum calculations and with ASEP/MD



however, any information about inhomogeneous bandwidth is missing during the averaging procedure. The execution of hundreds or thousands of quantum calculations in order to obtain the inhomogeneous bandwidth or any other property is contrary to the MFA philosophy, where only a limited number of quantum calculation is required. For this reason, a new procedure has been designed, in the context of ASEP/MD, with the aim of making an estimation of the bandwidth. The procedure was described in the Sect. 2. In order to confirm its validity, the statistical distribution of the transition energies obtained from 100 quantum calculations is compared with that obtained with the new procedure. We present here the results obtained for two molecules, one polar and the other non-polar, acrolein and *p*-DFB, respectively, both in water solution.

For acrolein, the histograms of the statistical distribution of the excitation energies obtained from the 100 quantum calculations set and with ASEP/MD are shown in Fig. 3. The small differences between the two methods can be associated with the SSE, i.e., the use of averaged solute wave function instead of a fluctuating one in the determination of the solute–solvent interaction energies. In ASEP/MD, the solute molecule does not polarize in response to thermal instantaneous changes in the solvent structure. For acrolein, the two methods provide the same standard deviation, 2.81 kcal/mol . In *p*-DFB, the agreement is also very good; the distribution of quantum transition energies has a standard deviation of 0.27 kcal/mol while the ASEP/MD distribution yields a value of 0.26 kcal/mol . Regarding the interaction energy distributions for the ground and excited state, in this case the agreement between the values provided by the two methods is somewhat worse, but the results are still satisfactory. In the two molecules, the statistical dispersion is lower for the excited state than for the ground state, and this trend is especially important in acrolein, probably as a consequence of the large dipole moment decreasing during the excitation.

Fig. 4 **a** RDFs corresponding to the pair Ow-O (water oxygen-solute carboxylic oxygen), for acrolein and formaldehyde, and Ow-F (water oxygen-solute fluorine), for *p*-DFB and *trans*-DFE. Full line for Ow-O of acrolein, dotted line for Ow-O of formaldehyde, dashed line for Ow-F of t-DEF and dash-dotted line for Ow-F of p-DFB. **b** The equivalent RDFs with the water hydrogens ($Rdf(Hw-O)$) and $Rdf(Hw-F)$. Full line for Hw-O of acrolein, dotted line for Hw-O of formaldehyde, dashed line for Hw-F of t-DEF and dash-dotted line for Hw-F of p-DFB



It is also worth indicating that although polar solutes yield more structured solvents (characterized by RDFs with higher peaks), the dispersion of the solute–solvent interaction energies is wider (because small changes at the solvent position greatly modify the solute–solvent interaction energies). See Sect. 4.4 for more details.

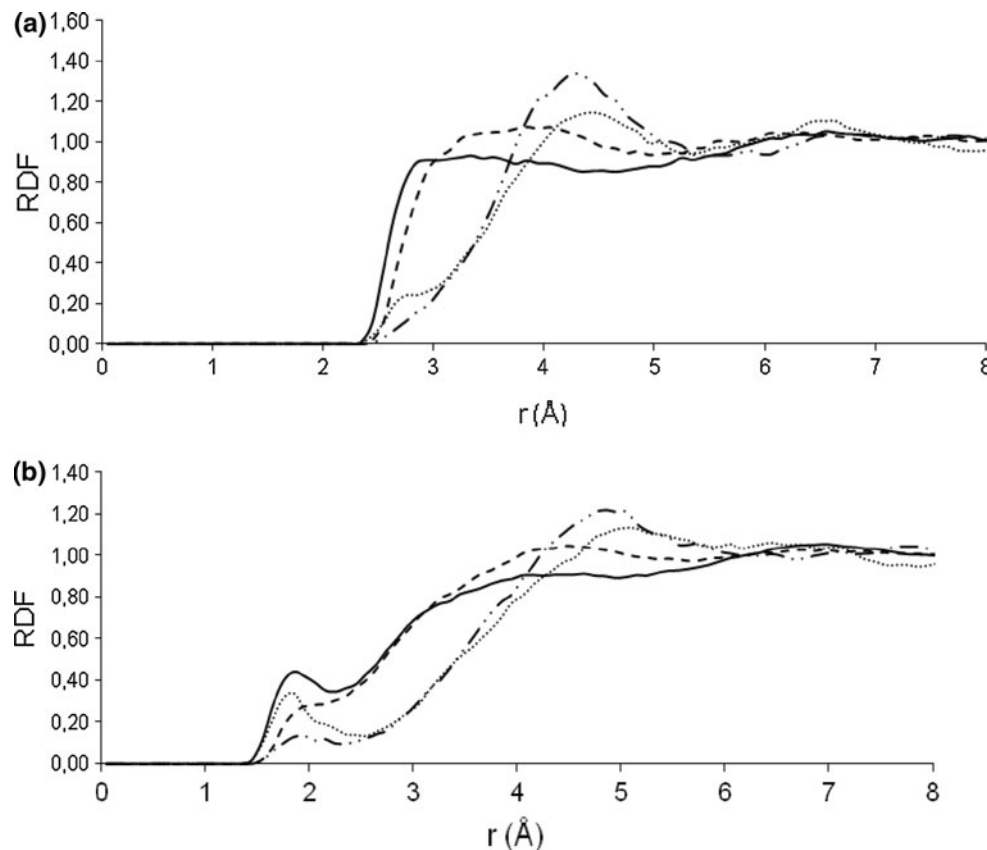
In sum, the procedure proposed permits to account for most of the inhomogeneous bandwidth broadening. This means that ASEP/MD can be easily employed in the estimation of the bandwidth with almost no additional computational cost, correcting one of the main shortcomings of the MFA.

4.4 Solvent structure

Figures 4 and 5 display some of the most important radial distribution functions (RDF) for the solute–solvent interaction. In particular, Fig. 4a collects the RDFs corresponding to the pair Ow-O (water oxygen–solute carboxylic oxygen), for acrolein and formaldehyde, and Ow-F (water oxygen–solute fluorine) for *p*-DFB and *trans*-DFE. The interactions with the water hydrogens [$Rdf(Hw-O)$

and $Rdf(Hw-F)$] are represented in Fig. 4b. It can be observed a great difference between the solvent distribution of the water molecules around acrolein and formaldehyde with respect to the distribution around *p*-DFB and *trans*-DFE. As a consequence of a more effective interaction, polar molecules get a more structured solvent distribution and very defined peaks around 1.8 and 2.7 Å, corresponding to the first solvation shell for $Rdf(Hw-O)$ and $Rdf(Ow-O)$, respectively, are clearly recognized. Although for *p*-DFB and *trans*-DFE, the water structure is practically negligible, in Fig. 4b it can be distinguished for them a weak shoulder that appears at the same position as the first peak for acrolein and formaldehyde. Figure 5 collects the RDFs corresponding to the pairs O(s)-F and H(s)-F for *p*-DFB and *trans*-DFE in water and in methanol. O(s) and H(s) represent the oxygen and hydrogen atoms when the solvent is water and the hydroxyl oxygen and hydrogen atoms when solvent is methanol. Given the non-polar nature of *p*-DFB and *trans*-DFE, their RDFs are very similar, independently of the solvent, water or methanol, considered. The RDFs do not display well-defined peaks in these cases.

Fig. 5 RDFs corresponding to the pairs O(s)-F and H(s)-F for *p*-DFB and *trans*-DFE in water and in methanol. O(s) and H(s) represent the oxygen and hydrogen atoms when the solvent is water and the hydroxylic oxygen and hydrogen atoms when solvent is methanol. **a** O solvent—F solute. *Full line* for *p*-DFB in water, *dotted line* for *p*-DFB in methanol, *dashed line* for *t*-DFE in water and *dash-dotted line* for *t*-DFE in methanol. **b** H solvent—F solute. *Full line* for *p*-DFB in water, *dotted line* for *p*-DFB in methanol, *dashed line* for *t*-DFE in water and *dash-dotted line* for *t*-DFE in methanol



5 Conclusions

In this paper, we have tackled the influence that solvent Stark effect has on the electron spectra appearance and excited states properties. Four molecules, two polar (acrolein and formaldehyde) and two non-polar (*p*-DFB and *trans*-DFE), have been studied in three solvents of different polarity using the ASEP/MD methodology. As expected, the solvent shift in the absorption energies increases with the polarity of the solute and solvent passing from only 0.2 kcal/mol for *p*-DFB in cyclohexane to 5.2 kcal/mol for acrolein in water solution. No significant influence has been noted on the optimized geometries, transition energies or solvent shift values with the different level of calculations (MP2 or CASSCF) or the different active spaces used with CASSCF method.

Independently of the system considered, the conclusions have been similar: SSE does not have an appreciable effect on the solvent shift or on the multipole moment values. In the case of the solvent shifts, the contribution of the SSE remains lower than 0.06 kcal/mol even in polar systems. Such a small contribution is consequence of the cancellation of the solvent Stark contributions to the solute–solvent interaction energy in the ground and excited states. Since the SSE values provide also a measure of the errors

introduced by MFA, these results indicate that MFA is a very good approximation that permits an accurate determination of the solvent shift at the same time that it reduces drastically the computational cost. The same conclusion can be extracted from the analysis of the dipole and quadrupole moments both in the ground and the excited states.

Our results permit discarding the SSE as cause of the solvent shift in centro-symmetric molecules, which must be assigned to the electrostatic interaction of solute quadrupole and higher multipole moments with the solvent.

Finally, a new procedure has been proposed for the calculation of the inhomogeneous bandwidth broadening of electronic transitions in an efficient way suited to the ASEP/MD methodology. The statistical distributions of the transition energies obtained from 100 quantum calculations are compared with those provided by ASEP/MD. Both statistical distributions show almost coincident characteristics for acrolein and *p*-PFB in water solution. It can be concluded that the method proposed recovers most of the inhomogeneous bandwidth broadening of electronic transitions for polar and non-polar systems.

Acknowledgments This work was supported by the CTQ2008-06224 Project from the Ministerio de Ciencia e Innovación of Spain and the PRI08A056 Project from the Consejería de Economía, Comercio e Innovación of the Junta de Extremadura.

References

1. Linder B (1967) *Adv Chem Phys* 12:225
2. Karlstrom G, Halle B (1993) *J Chem Phys* 99:8056
3. Ghoneim N, Suppan P (1995) *Spectrochim Acta* 51A:1043
4. Gosh AS, Basu S (1974) *J Photochem* 3:247
5. Tomasi J, Persico M (1994) *Chem Rev* 94:2027
6. Tomasi J, Mennucci B, Cammi R (2005) *Chem Rev* 105:2999
7. Tapia O, Goscinski O (1975) *Mol Phys* 29:1653
8. Orozco M, Luque FJ (2000) *Chem Rev* 100:4187
9. Rivail JL, Rinaldi D (1995) In: Leszczynski J (ed) Computational chemistry: review of current trends. World Scientific Publishing, Singapore
10. Cramer CJ, Truhlar CJ (1995) In: Lipkowitz KB, Boyd DB (eds) Reviews in computational chemistry, vol VI. VCH Publishers, New York
11. Cramer CJ, Truhlar DG (1999) *Chem Rev* 99:2161
12. Warshel A (1991) Computer modelling of chemical reactions in enzymes and solutions. Wiley-Interscience, New York
13. Warshel A, Levitt M (1976) *J Mol Biol* 103:227
14. Field MJ, Bash PA, Karplus M (1990) *J Comput Chem* 11:700
15. Luzhkov V, Warshel A (1992) *J Comput Chem* 13:199
16. Gao J (1992) *J Phys Chem* 96:537
17. Wei D, Salahub DR (1994) *Chem Phys Lett* 224:291
18. Tuñón I, Martins-Costa MTC, Millot C, Ruiz-López MF, Rivail JL (1996) *J Comput Chem* 17:19
19. Wesolowski TA, Warshel A (1993) *J Phys Chem* 97:8050
20. Stanton RV, Little LR, Merz KM (1995) *J Phys Chem* 99:17344
21. Gao J, Truhlar DG (2002) *Annu Rev Phys Chem* 53:467
22. Ten-no S, Hirata F, Kato S (1994) *J Chem Phys* 100:7443
23. Allen MP, Tildesley DJ (1987) Computer simulation of liquids. Oxford University Press, London
24. McCammon JA, Harvey JC (1987) Dynamics of proteins and nucleic acids. Cambridge University Press, Cambridge
25. Fdez. Galván I, Sánchez ML, Martín ME, Olivares del Valle FJ, Aguilar MA (2003) *Comput Phys Commun* 155:244
26. Fdez. Galván I, Olivares del Valle FJ, Martín ME, Aguilar MA (2004) *Theor Chem Acc* 111:196
27. Fdez. Galván I, Aguilar MA, Ruiz-López MF (2005) *J Phys Chem B* 109:23024
28. Muñoz-Losa A, Martín ME, Fdez. Galván I, Aguilar MA (2007) *Chem Phys Lett* 443:76
29. Muñoz-Losa A, Fdez. Galván I, Sánchez ML, Martín ME, Aguilar MA (2008) *J Phys Chem B* 112:877
30. Muñoz-Losa A, Fdez. Galván I, Martín ME, Aguilar MA (2006) *J Phys Chem B* 110:18064
31. Martín ME, Sánchez ML, Olivares del Valle FJ, Aguilar MA (2000) *J Chem Phys* 113:6308
32. Muñoz-Losa A, Fdez. Galván I, Aguilar MA, Martín ME (2008) *J Phys Chem B* 112:8815
33. Martín ME, Muñoz-Losa A, Fdez. Galván I, Aguilar MA (2004) *J Chem Phys* 121:3710
34. Sánchez ML, Aguilar MA, Olivares del Valle FJ (1997) *J Comput Chem* 18:313
35. Sánchez ML, Martín ME, Aguilar MA, Olivares del Valle FJ (2000) *J Comput Chem* 21:705
36. Martín ME, Sánchez ML, Olivares del Valle FJ, Aguilar MA (2002) *J Chem Phys* 116:1613
37. Sánchez ML, Martín ME, Fdez. Galván I, Olivares del Valle FJ, Aguilar MA (2002) *J Phys Chem B* 106:4813
38. Yamamoto T (2008) *J Chem Phys* 129:244104
39. Frisch MJ, Trucks GW, Schlegel HB, Scuseria GE, Robb MA, Cheeseman JR, Zakrzewski VG, Montgomery JA Jr, Stratmann RE, Burant JC, Dapprich S, Millam JM, Daniels AD, Kudin KN, Strain MC, Farkas O, Tomasi J, Barone V, Cossi M, Cammi R, Mennucci B, Pomelli C, Adamo C, Clifford S, Ochterski J, Petersson GA, Ayala PY, Cui Q, Morokuma K, Malick DK, Rabuck AD, Raghavachari K, Foresman JB, Cioslowski J, Ortiz JV, Baboul AG, Stefanov BB, Liu G, Liashenko A, Piskorz P, Komaromi I, Gomperts R, Martin RL, Fox DJ, Keith T, Al-Laham MA, Peng CY, Nanayakkara A, Gonzalez C, Challacombe M, Gill PMW, Johnson B, Chen W, Wong MW, Andres JL, Gonzalez C, Head-Gordon M, Replogle ES, Pople JA (1998) Gaussian 98. Gaussian Inc, Pittsburgh
40. Refson K (2000) *Comput Phys Commun* 126:310
41. Møller C, Plesset MS (1934) *Phys Rev* 46:618
42. Roos BO (1987) In: Lawley KP (ed) Ab initio methods in quantum chemistry. Wiley, New York
43. Roos BO, Fülscher MP, Malmqvist PÅ, Merchán M, Serrano-Andrés L (1994) In: Langhorff SR (ed) Quantum mechanical electronic structure calculations with chemical accuracy. Kluwer, Dordrecht
44. Andersson K, Malmquist PÅ, Roos BO (1992) *J Chem Phys* 96:1218
45. Malmquist PÅ, Roos BO (1989) *Chem Phys Lett* 155:189
46. Andersson K, Barysz M, Bernhardsson A, Blomberg MRA, Carissan Y, Cooper DL, Cossi M, Fleig T, Fülscher MP, Gagliardi L, de Graaf C, Hess BA, Karlström G, Lindh R, Malmqvist PÅ, Neogrády P, Olsen J, Roos BO, Schimmelpfennig B, Schütz M, Seijo L, Serrano-Andrés L, Siegbahn PEM, Stalring J, Thorsteinsson T, Veryazov V, Wierzbowska M, Widmark PO (2003) MOLCAS, version 6.2. University of Lund, Lund
47. Jorgensen WL, Maxwell DS, Tirado-Rives J (1996) *J Am Chem Soc* 118:11225
48. Jorgensen WL, Chandrasekhar J, Madura JD, Impey RW, Klein ML (1983) *J Chem Phys* 79:926
49. Hoover WG (1985) *Phys Rev A* 31:1695
50. Brand JCD, Williamson DG (1963) *Discuss Faraday Soc* 35:184
51. Becker RS, Inuzuka K, King J (1970) *J Chem Phys* 52:5164
52. Walzl KN, Koerting CF, Kuppermann A (1987) *J Chem Phys* 87:3796
53. Robin MB (1985) In: Higher excited states of polyatomic molecules, vol 3. Academic Press, New York
54. Sponer H (1954) *J Chem Phys* 22:234
55. Belanger G, Sandorfy C (1971) *J Chem Phys* 55:2055
56. González-Vázquez J, González L (2008) *Chem Phys* 349:287